Quantum Monte Carlo study of electrostatic potential in graphene

N. Yu. Astrakhantsev,[1,2,*] V. V. Braguta,[1,2,4,5,†] M. I. Katsnelson,[6,7] A. A. Nikolaev,[1,3] and M. V. Ulybyshev[8]

[1]*Institute of Theoretical and Experimental Physics, 117218 Moscow, Russia*

[2]*Moscow Institute of Physics and Technology, Institutskii per. 9, Dolgoprudny, Moscow Region, 141700 Russia*

[3]*Far Eastern Federal University, School of Biomedicine, 690950 Vladivostok, Russia*

[4]*Institute for High Energy Physics NRC "Kurchatov Institute," Protvino, 142281 Russian Federation*

[5]*Bogoliubov Laboratory of Theoretical Physics, Joint Institute for Nuclear Research, 141980 Dubna, Russia*

[6]*Radboud University, Institute for Molecules and Materials, Heyendaalseweg 135, NL-6525AJ Nijmegen, The Netherlands*

[7]*Ural Federal University, Theoretical Physics and Applied Mathematics Department, Mira Str. 19, 620002 Ekaterinburg, Russia*

[8]*Institute of Theoretical Physics, University of Regensburg, Regensburg, Universitatsstrasse 31, D-93053, Germany*

(Received 2 October 2017; published 4 January 2018)

In this paper the interaction potential between static charges in suspended graphene is studied within the quantum Monte Carlo approach. We calculated the dielectric permittivity of suspended graphene for a set of temperatures and extrapolated our results to zero temperature. The dielectric permittivity at zero temperature is found to have the following properties. At zero distance $\epsilon = 2.24 \pm 0.02$. Then it rises and at a large distance the dielectric permittivity reaches the plateau $\epsilon \simeq 4.20 \pm 0.66$. The results obtained in this paper allow us to draw a conclusion that full account of many-body effects in the dielectric permittivity of suspended graphene gives ϵ very close to the one-loop results. Contrary to the one-loop result, the two-loop prediction for the dielectric permittivity deviates from our result. So one can expect large higher order corrections to the two-loop prediction for the dielectric permittivity of suspended graphene.

DOI: 10.1103/PhysRevB.97.035102

I. INTRODUCTION

Graphene, a two-dimensional crystal composed of carbon atoms packed in a honeycomb lattice [1,2], attracts considerable interest because of its electronic properties. There are two Fermi points in the electronic spectrum of graphene. In the vicinity of each point the fermion excitations are similar to the massless Dirac fermions living in two dimensions [3–6]. The relativistic nature of fermion excitations in graphene leads to numerous quantum relativistic phenomena such as Klein tunneling, minimal conductivity through evanescent waves, relativistic collapse at a supercritical charge, etc. [7–9].

The Fermi velocity in graphene is much smaller than the speed of light ($v_F \sim c/300$), resulting in negligible retardation effects and magnetic interactions between quasiparticles. Thus the interaction in graphene can be approximated by the instantaneous Coulomb potential with the large effective coupling constant $\alpha_{\text{eff}} = \alpha \cdot c/v_F \sim 300/137 \sim 2.2$.

It is reasonable to assume that the observables in graphene theory are considerably renormalized due to strong interaction as compared to noninteracting theory. For instance, the leading perturbative renormalization of the Fermi velocity with the logarithmic accuracy [10–14] leads to increase of v_F as large as $\sim$100% for the suspended graphene. One can expect that higher order renormalization leads to further considerable change of the bare value of the Fermi velocity. However, existing experimental measurements of the Fermi velocity [15,16] are in a good agreement with the first-order perturbation theory improved by the one-loop expression for the dielectric permittivity of graphene. Recently it was shown that the next-to-leading-order corrections in the random phase approximation (RPA) are small relative to the leading-order RPA results [17]. Nevertheless, it is not clear what happens to the perturbative corrections after the next-to-leading order.

Another important observable in graphene is the interaction potential between static charges. The renormalization of the static potential can be parametrized by the dielectric permittivity which depends on the distance between static charges $\epsilon(r)$. One-loop expression for $\epsilon(r)$ was calculated in [18]. At small distances $\epsilon(r) \sim 2$. Then the dielectric permittivity grows with the distance and at large distances $r \gg a$[1] it reaches the well known one-loop expression [8,9]

$$\epsilon = 1 + \frac{\pi}{2}\alpha_{\text{eff}}. \tag{1}$$

For $\alpha_{\text{eff}} = 2.2$ this formula gives $\epsilon = 4.4$. So one sees that the one-loop correction is very large. The two-loop correction to ϵ was calculated in [19] and can be written as

$$\epsilon = 1 + \frac{\pi}{2}\alpha_{\text{eff}} + 0.778\alpha_{\text{eff}}^2. \tag{2}$$

If one takes $\alpha_{\text{eff}} = 2.2$ the dielectric permittivity is $\epsilon = 8.2$. If one accounts for one-loop renormalization of α_{eff} (see below), $\epsilon \simeq 2.5$. So it is clear that the next-to-leading-order corrections considerably modify the one-loop result. One can also expect that higher order corrections are also important.

In this paper we are going to study the interaction potential between static charges in suspended graphene within quantum

*astrakhantsev@itep.ru

†braguta@itep.ru

[1]The a is the distance between carbon atoms in graphene.

Monte Carlo simulations. There are a lot of papers where a quantum Monte Carlo approach was used to study graphene properties [20–26]. The first Monte Carlo study of the static interaction potential based on the low energy effective theory of graphene was done in Ref. [27]. In this paper we are going to use the approach which is based on the tight-binding Hamiltonian without the expansion near the Fermi points [26]. This approach allows us to avoid ambiguity due to regularization procedure. In addition, the interactions between quasiparticles are parametrized by the realistic phenomenological potential obtained in Ref. [28], which significantly deviates from the Coulomb potential at small distances. However, the main advantage of the Monte Carlo approach is that it fully accounts for interactions between quasiparticles based on first principles.

This paper is organized as follows. In the next section we briefly describe the method of lattice Monte Carlo simulation of graphene. Section III is devoted to the discussion of how the potential of static charges can be calculated within Monte Carlo simulations. The results of the calculation are presented in Sec. IV. In the last section we summarize our results.

II. BRIEF DESCRIPTION OF THE MODEL

In the calculation we use the tight-binding model of graphene. The Hamiltonian consists of the tight-binding term and the interaction part describing the full electrostatic interaction between quasiparticles:

$$\begin{aligned}\hat{H} = &-\kappa \sum_{\langle x,y\rangle} (\hat{a}^\dagger_{y,\uparrow}\hat{a}_{x,\uparrow} + \hat{a}^\dagger_{y,\downarrow}\hat{a}_{x,\downarrow} + \text{H.c.}) \\ &+ \sum_{x=\{1,\xi\}} m(\hat{a}^\dagger_{x,\uparrow}\hat{a}_{x,\uparrow} - \hat{a}^\dagger_{x,\downarrow}\hat{a}_{x,\downarrow}) \\ &- \sum_{x=\{2,\xi\}} m(\hat{a}^\dagger_{x,\uparrow}\hat{a}_{x,\uparrow} - \hat{a}^\dagger_{x,\downarrow}\hat{a}_{x,\downarrow}) \\ &+ \frac{1}{2}\sum_{x,y} V_{xy}\hat{q}_x\hat{q}_y, \end{aligned} \tag{3}$$

where $\kappa = 2.7$ eV is the hopping between nearest neighbors, and $\hat{a}^\dagger_{x,\uparrow}$, $\hat{a}_{x,\uparrow}$ and $\hat{a}^\dagger_{x,\downarrow}$, $\hat{a}_{x,\downarrow}$ are creation/annihilation operators for spin-up and spin-down electrons at π orbitals. Spatial index $x = \{s,\xi\}$ consists of sublattice index $s = 1,2$ and the two-dimensional coordinate $\xi = \{\xi_1,\xi_2\}$ of the unit cell in rhombic lattice. Periodical boundary conditions are imposed in both spatial directions in the same manner as in [26]. The mass term has a different sign at different sublattices. According to our algorithm, we should introduce mass in order to eliminate zero modes from the fermionic determinant. The calculation is carried out at few various masses and final results are obtained through the chiral extrapolation $m \to 0$.

The matrix V_{xy} is the bare electrostatic interaction potential between sites with coordinates x and y and $\hat{q}_x = \hat{a}^\dagger_{x,\uparrow}\hat{a}_{x,\uparrow} + \hat{a}^\dagger_{x,\downarrow}\hat{a}_{x,\downarrow} - 1$ is the electric charge operator at lattice site x. The potential V_{xy} represents screened Coulomb interaction. At small distances $r/a \leqslant 2$ we employ phenomenological potentials V_{00}, V_{01}, V_{02}, V_{03} calculated in [28], while at distances $r/a \geqslant 2$ we use the Coulomb-like potential

$$V(r) = \frac{A}{r/a + C}, \tag{4}$$

where $A = \alpha \cdot \hbar c/a = 10.14$ eV, $C = 0.82$. The parameter C is chosen so that $V(2a) = V_{03}$. This choice ensures smooth interpolation between regions of the phenomenological potential and the Coulomb-like potential.

All calculations were performed using the hybrid Monte Carlo algorithm. Details of the algorithm are described in [26]. The method is based on the Suzuki-Trotter decomposition. Partition function $\exp(-\beta\hat{H})$ is represented in the form of a functional integral in Euclidean time. Inverse temperature is equal to the number of time slices multiplied by the step in Euclidean time: $\delta\tau L_t = \beta = 1/T$. Since the algorithm requires fermionic fields to be integrated out, we eliminate all four fermionic terms in the full Hamiltonian using the Hubbard-Stratonovich transformation. The final form of the partition function can be written as

$$\text{Tr}\, e^{-\beta\hat{H}} \cong \int \mathcal{D}\varphi_{x,n} e^{-S[\varphi_{x,n}]} |\det M[\varphi_{x,n}]|^2. \tag{5}$$

$\varphi_{x,n}$ is the Hubbard-Stratonovich field for time slice n and spatial coordinate x. A particular form of the fermionic operator M is described in [26]. The absence of the sign problem (appearance of the squared modulus of the determinant) is guaranteed by the particle-hole symmetry in graphene at the neutrality point. Action for the Hubbard field $S[\varphi_{x,n}]$ is also a positively defined quadratic form for all variants of electron-electron interaction used in our paper. Thus we can generate configurations of $\varphi_{x,n}$ by the Monte Carlo method using the weight (5) and calculate physical quantities as averages over generated configurations.

III. DETAILS OF THE CALCULATION

To calculate the potential of the static charges in graphene one introduces the Polyakov loop of the Hubbard-Stratonovich field. The Polyakov loop is defined as a product of the factors[2] $\exp(iQ\delta\tau\varphi_{\vec{x},t})$ over all slices in Euclidean time t and with fixed spatial coordinate $\vec{x}$,

$$L_Q(\vec{x}) = \prod_{t=0}^{L_t-1} \exp(-iQ\Delta\tau\varphi_{\vec{x},t}). \tag{6}$$

Physically the introduction of the operator $L_Q(\vec{x})$ implies the calculation of the partition function of graphene with the static charge Q,

$$\langle L_Q\rangle = \exp(-F_Q/T), \tag{7}$$

where F_Q is the free energy of the static charge Q in graphene.

Similarly the correlation function of the Polyakov loops $\langle L_Q(0)L^*_Q(\vec{r})\rangle$ is determined by the free energy of static charges Q and $-Q$ separated by the distance $\vec{r}$. The free energy of this system is determined by the potential of the static charges in graphene $V_{QQ}(\vec{r})$. Thus we have

$$\langle L_Q(0)L^*_Q(\vec{r})\rangle \sim \exp[-V_{QQ}(\vec{r})/T]. \tag{8}$$

In order to obtain an interaction potential we use the following relation:

$$V_{QQ}(\vec{r}) = -\frac{T}{Q^2}[\ln\langle L_Q(0)L^*_Q(\vec{r})\rangle - 2\ln\langle L_Q\rangle]. \tag{9}$$

[2]Notice that the charge Q is measured in units of electron charge e.

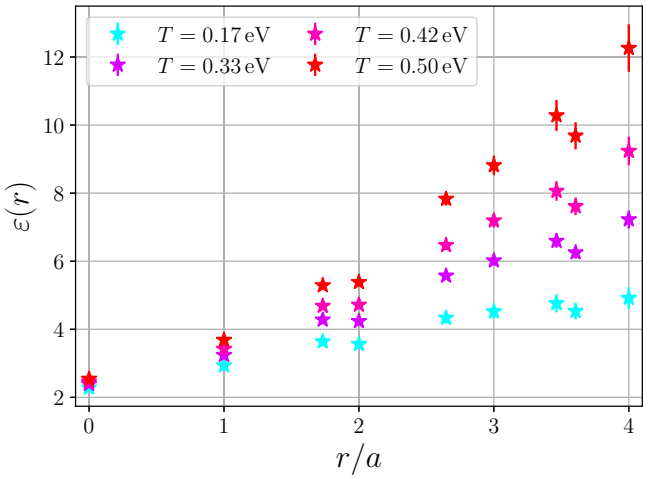

FIG. 1. The dielectric permittivity of graphene $\epsilon(r,T)$ as a function of distance r/a for the $T = 0.167$, 0.333, 0.417, and 0.50 eV.

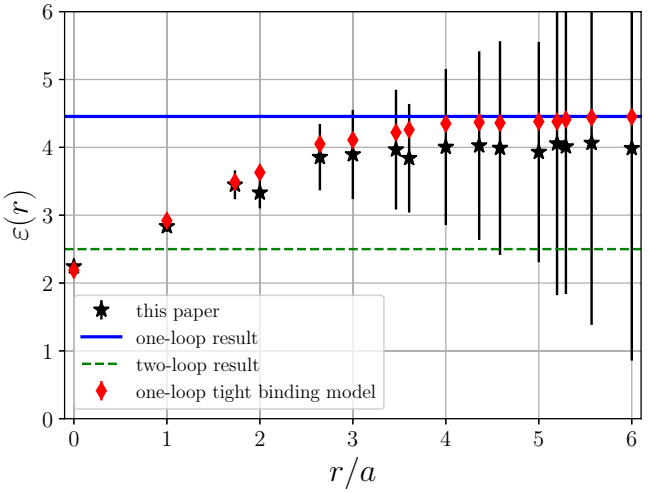

FIG. 2. The dielectric permittivity of suspended graphene $\epsilon(r)$ as a function of distance r/a at zero temperature. The results obtained in this paper are represented by black star points. The blue line and green dashed line correspond to the one-loop result (1) and the two-loops result (2), correspondingly. The red diamond points correspond to the one-loop calculation of the $\epsilon(r)$ based on tight-binding model (3) carried out in [18].

In the simulations one can take an arbitrary (but not too large) value of the static charge Q. In [27] it was shown that within the uncertainty of calculations the results do not depend on Q. However, it turns out that the signal-to-noise ratio significantly depends on the value of Q. This dependence was studied in [27] and it was shown that the value $Q = 0.1$ is appropriate for the calculation of the potential with a good signal-to-noise ratio. For this reason the calculations in this paper are carried out at $Q = 0.1$.

Monte Carlo simulation of graphene was carried out on the lattices with spatial extension $L_x = L_y = 30$. The lattice spacing in temporal direction is $\delta\tau = 0.1$ eV. The temporal sizes of the lattices under study are $L_t = 60, 50, 36, 34, 30, 26, 24, 22, 20$ which correspond to the temperatures $T = 0.167, 0.2, 0.278, 0.294, 0.333, 0.385, 0.417, 0.455, 0.5$ eV. For the lattices $30^2 \times 36 \cdots 20$ we conducted the calculations at the following values of the fermion mass $m = 0.03, 0.05, 0.07, 0.1$ eV. For the two lowest temperatures on the lattices $30^2 \times 60$ and $30^2 \times 50$ the fermion masses are $0.01, 0.02, 0.03, 0.04$ eV. For these values of the fermion masses we simulate relativistic fermions. To obtain the results for the massless fermions we fit our data for all temperatures and distances under study by the function $V_{QQ}(r) = V_0(r) + V_1(r)m^2$. For all temperatures and distances the data are well described by this fit ($\chi^2 \leqslant 1$). The function $V_0(r)$ gives the potential in the massless limit. Below we present the results obtained in the limit of massless fermions $m \to 0$.

IV. RESULTS OF THE CALCULATION

In Fig. 1 we present the results of the calculation of the dielectric permittivity of graphene $\epsilon(r)$ which is the ratio of bare potential (4) to the one measured on the lattice (9). The dielectric permittivity is presented as a function of distance r/a for the temperatures $T = 0.167, 0.333, 0.417, 0.5$ eV. Similar plots can be shown for the other temperatures under consideration.

It is seen from Fig. 1 that the $\epsilon(r)$ rises with the distance. Moreover, the larger the temperature the sharper the rise of the dielectric permittivity. We believe that this behavior can be attributed to the Debye screening in graphene at nonzero temperature. In order to get rid of the Debye screening effect and find the dielectric permittivity at zero temperature we are going to fit dielectric permittivity at every fixed distance with the anzatz

$$\varepsilon(r,T) = A(r) + B(r)T + C(r)T^2. \tag{10}$$

In conducting the fitting procedure we impose a constrain $B(r) > 0$. Physically this constrain is motivated by the requirement that at $T \to 0$ and $T \neq 0$ Debye screening effect diminishes the potential, i.e., enhances the value of the dielectric permittivity. The coefficient $A(r)$ in the last equation gives the dielectric permittivity of suspended graphene at zero temperature $\varepsilon(r, T = 0)$. In Fig. 2 and Table I we present the $\varepsilon(r, T = 0)$ as a function of distance r/a.

TABLE I. The dielectric permittivity of suspended graphene $\epsilon(r)$ as a function of distance r/a at zero temperature. The first column is the distance in graphene lattice units. The second column is the $\epsilon(r)$ calculated in this paper. The third column contains the $\epsilon(r)$ calculated at one-loop level of the tight-binding model (3).

r/a	$\varepsilon(r)$	$\varepsilon_{1\,\mathrm{loop}}(r)$
0.00	2.24 ± 0.02	2.19
1.00	2.83 ± 0.08	2.92
1.73	3.45 ± 0.21	3.49
2.00	3.33 ± 0.23	3.63
2.65	3.86 ± 0.49	4.05
3.00	3.89 ± 0.66	4.11
3.46	3.97 ± 0.88	4.22
3.61	3.84 ± 0.80	4.26
4.00	4.01 ± 1.15	4.35

From Fig. 2 and Table I it is seen that the dielectric permittivity at the $r = 0$ is $\epsilon = 2.24 \pm 0.02$. Then it rises and after $r/a \geqslant 3$ the dielectric permittivity comes out to the plateau $\epsilon(r) \simeq 4$. It is seen that the uncertainties of the calculation rise with the distance from rather small values to large ones. The uncertainties at distances $r/a \geqslant 6$ become very large for this reason and we do not show these points in Fig. 2.

The main reason for large uncertainties of the calculation at large distance is the Debye screening at nonzero temperature in graphene. In order to find the value of the dielectric permittivity at large distance with better accuracy we have to account for the Debye screening effect.

We are going to do this as follows. The Debye screening of the Coulomb potential in graphene was calculated in [18,27] and it is given by the formula

$$V(r) = \frac{Q}{\tilde{\epsilon} r} \int_0^\infty d\xi \frac{e^{-(m_D r)\xi}}{(1+\xi^2)^{3/2}}, \tag{11}$$

where $\tilde{\epsilon}$ is the dielectric permittivity and the m_D is the Debye mass. We fit our data for each temperature under consideration with the parameters $\tilde{\epsilon}$ and m_D. Thus we get rid of the Debye screening effect which enhances the uncertainty at large distance. Notice that our bare potential deviates from Coulomb (4) and tends to it only at large distance.

In the fitting procedure we study the potential $V(r)$ in the region $r/a \in [4,8]$. We chose this reason for the following reasons. First, if one extends the region where our data are fitted to larger distance we will get larger uncertainties of the calculation. Second, within this region the deviation from the Coulomb potential is already sufficiently small ∼10%–20%. Formula (11) describes our data quite well ($\chi^2/dof \sim 1$) for all temperatures and allows one to determine $\tilde{\epsilon}(T)$ as a function of temperature.

To proceed we fit the results for the $\tilde{\epsilon}$ by the function $\tilde{\epsilon}(T) = \tilde{A} + \tilde{B}T + \tilde{C}T^2$. The value of the $\tilde{A}$ gives the dielectric permittivity at zero temperature and large distance. Thus we obtain

$$\epsilon = 4.20 \pm 0.66. \tag{12}$$

In the formula (12) we accounted for statistical uncertainty and the uncertainty due to the deviation of the potential (4) from Coulomb. More detailed description of the fitting procedure can be found in the Appendix.

Furthermore, let us proceed to the comparison of the results obtained in this paper with the perturbative expressions for the dielectric permittivity of suspended graphene. In Fig. 2 we present the results of one-loop calculations of the dielectric permittivity. The red diamond points correspond to the one-loop dielectric permittivity calculated within the tight-binding model (3) in [18]. The blue line corresponds to the one-loop result (1) which is obtained within the effective theory of graphene. It is seen that the full account of many-body effects in the dielectric permittivity of suspended graphene within Monte Carlo study gives $\epsilon(r)$ which is very close to the one-loop results. The value of $\epsilon(r)$ at large distance (12) also agrees with the one-loop result (1).

Here one comment is in order. In Ref. [18] the results for the dielectric permittivity calculated within different approaches are presented. In particular, in Fig. 10 of [18] the dielectric permittivity calculated within the tight-binding model, the leading-order RPA, and the quantum Monte Carlo approach (preliminary results) were presented. Notice that the interaction potential used in all these calculations differs from the potential (4) used in our paper on the Coulomb tail. In particular, at large distance the potential (4) behaves like $V(r) = \alpha\hbar c/r$ which differs from the behavior $V(r) = \alpha\hbar c/(1.4r)$ used in [18]. For this reason our results deviate mildly from the ones obtained in [18].

In Fig. 2 we also plot the results of [19] which is given by a two-loop formula (2). Since the calculation of the ϵ in [19] was carried at two loops, one has to renormalize the effective coupling constant α_{eff} at one loop in order to get the value of the dielectric permittivity. It is known that the renormalization of α_{eff} is reduced to the renormalization of the Fermi velocity v_R. It is rather difficult to find an unambiguous expression for v_R, since the renormalized Fermi velocity depends on the infrared scale and in the problem under consideration a lot of scales can play a role of the infrared scale.

To estimate ϵ at two loops we use the one-loop formula for v_R obtained in [18] and use temperature as the infrared scale:

$$v_F^R = v_F\left[1 + \frac{1}{4}\frac{\alpha}{(v_F/c)}\log\left(\frac{v_F\Lambda}{cT}\right)\right], \tag{13}$$

where v_F is the bare Fermi velocity, c is the speed of light, Λ is the ultraviolet cutoff, and T is the temperature which plays the role of the infrared scale in our estimation. In the calculation we take $v_F/c \sim 1/300$, $\Lambda \sim \hbar c/a$, and $T = 0.1$ eV which is a typical scale at which the calculations of this paper are carried out. With these numerical parameters we get $\epsilon = 2.5$. If we carry out the calculation at the room temperature $T = 293$ K, the two-loop dielectric permittivity is $\epsilon = 2.2$.

One can estimate the two-loop result for ϵ as it was proposed in Ref. [19]. The authors of this paper used the momentum $q \sim \hbar/r$ as an infrared scale in the renormalization of the Fermi velocity. It is clear that in the limit $r \to \infty$, $\alpha_{\text{eff}} \to 0$ and $\epsilon \to 1$. Notice that this limit is reached very slowly and one needs really huge graphene lattice to see that $\epsilon \simeq 1$. For this reason one can ask what is the typical two-loop dielectric permittivity on the lattice which is used in our calculation. To estimate it we use a typical distance on the lattices under consideration $L \sim 30a \sim \hbar/q$. In this case we get $\epsilon = 2.7$.

From this consideration one can state that all our estimations of the two-loop dielectric permittivity disagree with results obtained within the Monte Carlo method. So one can expect large higher order corrections to the two-loop result of [19].

V. CONCLUSION

In this paper the interaction potential between static charges in suspended graphene was studied within the quantum Monte Carlo simulations. This approach is based on the tight-binding Hamiltonian without the expansion near the Fermi points which allows us to avoid ambiguity due to the regularization procedure. In addition, the interactions between quasiparticles are parametrized by the realistic phenomenological potential, which deviates from the Coulomb potential at small distances. The main advantage of the Monte Carlo approach is that it fully accounts for interactions between quasiparticles based on first principles.

Within Monte Carlo simulations we calculated the dielectric permittivity of suspended graphene for a set of temperatures. For each distance between charges we carried out extrapolation to zero temperature. Thus we calculated the dielectric permittivity of suspended graphene at zero temperature.

We found that the behavior of the dielectric permittivity is the following. At zero distance $\epsilon = 2.24 \pm 0.02$. Then it rises and after $r/a \geqslant 3$ the dielectric permittivity comes out to the plateau $\epsilon(r) \simeq 4.20 \pm 0.66$. The results obtained in this paper allow one to draw a conclusion that the full account of many-body effects in the dielectric permittivity of suspended graphene gives the $\epsilon(r)$ that is very close to the one-loop results obtained analytically within the tight-binding model of graphene. The value of $\epsilon(r)$ at large distances also agrees with the one-loop calculation done within the low-energy effective theory of graphene.

We also found that the two-loop prediction for the dielectric permittivity deviates from the results of this paper. For this reason one can expect large higher order corrections to the two-loop prediction for the dielectric permittivity of suspended graphene.

Finally, we would like to stress the fact that the full account of many-body effects in the dielectric permittivity of suspended graphene, which gives the $\epsilon(r)$ close to the one-loop result, is highly nontrivial. The point is that the interaction in graphene is strong and it cannot be accounted for by perturbation theory. For instance, if we substitute the interaction potential (4) by Coulomb with the same A for all distance, graphene will turn from the semimetal phase to the insulator phase [22]. So it is not quite clear why two-loop and higher order corrections do not modify the dielectric permittivity considerably. From this perspective the dielectric permittivity of graphene is similar to the optical conductivity in graphene, where higher order many-body corrections are also not important [29].

ACKNOWLEDGMENTS

We would like to thank O. Pavlovsky who proposed us to use the bare potential from (4). The work of M.I.K. was supported by Act 211 Government of the Russian Federation, Contract No. 02.A03.21.0006. The work of M.V.U. was supported by DFG Grant No. BU 2626/2-1. The work of V.V.B. and A.Y.N., which consisted of numerical simulation and calculation of the static potential, was supported by a grant from the Russian Science Foundation (Project No. 16-12-10059). This work was carried out using high-performance computing resources of the federal center for collective usage at NRC Kurchatov Institute, http://computing.kiae.ru/. In addition, we used the supercomputer of Institute for Theoretical and Experimental Physics (ITEP).

APPENDIX

In this Appendix we give a detailed description of the fitting procedure giving the dielectric permittivity (12). To obtain the dielectric permittivity we fit our data by (11) for each temperature under consideration. In principle it is preferable to fit our data by (11) at large distances, because formula (11) describes Debye screening of the Coulomb potential and bare potential (4) approaches Coulomb only at sufficiently large distance. However, in practice it is difficult to calculate the static potential at very large distance since the uncertainty of the simulations grows with distance. So one should find a compromise between these constraints.

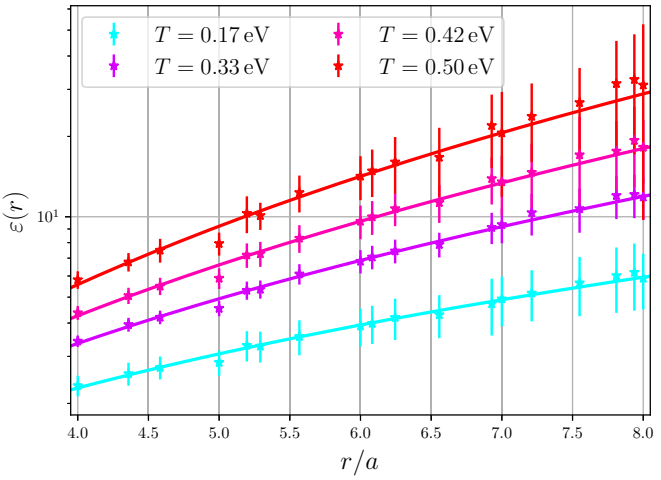

FIG. 3. The dielectric permittivity as a function of distance in the region $r/a \in [4,8]$ for the $T = 0.167$, 0.333, 0.417, and 0.50 eV. The curves represent the result of the fitting by (11).

In this paper we fit our data in the region $r/a \in [4,8]$. In this region the uncertainties are moderate and the deviation from the bare potential (4) is already sufficiently small. In Fig. 3 we plot the dielectric permittivity in the region $r/a \in [4,8]$ and the result of the fitting by (11) for a few temperatures.

The fitting by (11) gives $\tilde{\epsilon}$ and m_D. The values of these parameters for the temperatures under consideration are shown in Table II.

Having determined the values of the $\tilde{\epsilon}(T)$ we fit them with the function $\tilde{\epsilon}(T) = \tilde{A} + \tilde{B}T + \tilde{C}T^2$. The parameters of the fit are $\tilde{A} = 4.2 \pm 0.2$, $\tilde{B} = (-2.2 \pm 1.5)\ \mathrm{eV}^{-1}$, $\tilde{C} = (-5.0 \pm 2.3)\ \mathrm{eV}^{-2}$. The $\tilde{A}$ is the zero-temperature extrapolation of the dielectric permittivity.

The uncertainty of $\tilde{A}$ can be attributed to the statistical uncertainty of the numerical simulation. There is also a systematic uncertainty in $\tilde{A}$, appearing for the following reason. We fit our data by (11) which describes the Debye screening of the Coulomb potential. At the same time in the region $r/a \in [4,8]$ where we fit our data by (11) the deviation of the bare potential (4) from the Coulomb is

TABLE II. The parameters $\tilde{\epsilon}$ and m_D obtained from the fit of the potential by (11) for the temperatures under consideration.

T (eV)	m_D/T	$\tilde{\epsilon}$
0.17	318 ± 208	3.71 ± 0.86
0.20	393 ± 128	3.59 ± 0.55
0.28	475 ± 73	3.17 ± 0.32
0.33	575 ± 139	2.98 ± 0.57
0.38	734 ± 176	2.59 ± 0.60
0.42	784 ± 234	2.48 ± 0.75
0.45	919 ± 262	2.21 ± 0.72
0.50	1165 ± 462	1.77 ± 0.91

small but not negligible (∼10%–20%). In this paper we estimate this source of uncertainty as ∼15% of the dielectric permittivity.

Notice that the dielectric permittivity is the ratio of bare potential to the one measured on the lattice. Evidently the uncertainty due to the deviation from the Coulomb potential contributes both to the numerator and the denominator. Thus, there is a partial cancellation of these uncertainties and we believe it is overestimated in our paper. However, it is not clear how to estimate this uncertainty more accurately. Taking both statistical and systematic uncertainties into account we obtain the value of the dielectric permittivity at zero temperature:

$$\epsilon = 4.20 \pm 0.66. \tag{A1}$$

[1] K. S. Novoselov, A. K. Geim, S. V. Morozov, D. Jiang, Y. Zhang, S. V. Dubonos, I. V. Grigorieva, and A. A. Firsov, Science **306**, 666 (2004).

[2] A. K. Geim and K. S. Novoselov, Nat. Mater. **6**, 183 (2007).

[3] P. R. Wallace, Phys. Rev. **71**, 622 (1947).

[4] Y. Zhang, Y.-W. Tan, H. L. Stormer, and P. Kim, Nature (London) **438**, 201 (2005).

[5] G. W. Semenoff, Phys. Rev. Lett. **53**, 2449 (1984).

[6] K. S. Novoselov, A. K. Geim, S. V. Morozov, D. Jiang, M. I. Katsnelson, I. V. Grigorieva, S. V. Dubonos, and A. A. Firsov, Nature (London) **438**, 197 (2005).

[7] M. A. H. Vozmediano, M. I. Katsnelson, and F. Guinea, Phys. Rep. **496**, 109 (2010).

[8] V. N. Kotov, B. Uchoa, V. M. Pereira, F. Guinea, and A. H. C. Neto, Rev. Mod. Phys. **84**, 1067 (2012).

[9] M. I. Katsnelson, *Graphene: Carbon in Two Dimensions* (Cambridge University Press, Cambridge, 2012).

[10] J. Gonzalez, F. Guinea, and M. A. H. Vozmediano, Nucl. Phys. B **424**, 595 (1994).

[11] E. G. Mishchenko, Phys. Rev. Lett. **98**, 216801 (2007).

[12] I. F. Herbut, V. Juričić, and O. Vafek, Phys. Rev. Lett. **100**, 046403 (2008).

[13] L. Fritz, J. Schmalian, M. Muller, and S. Sachdev, Phys. Rev. B **78**, 085416 (2008).

[14] F. de Juan, A. G. Grushin, and M. A. H. Vozmediano, Phys. Rev. B **82**, 125409 (2010).

[15] D. C. Elias, R. V. Gorbachev, A. S. Mayorov, S. V. Morozov, A. A. Zhukov, P. Blake, L. A. Ponomarenko, I. V. Grigorieva, K. S. Novoselov, F. Guinea, and A. K. Geim, Nat. Phys. **7**, 701 (2011).

[16] G. L. Yu, R. Jalil, B. Belle, A. S. Mayorov, P. Blake, F. Schedin, S. V. Morozov, L. A. Ponomarenko, F. Chiappini, S. Wiedmann, U. Zeitler, M. I. Katsnelson, A. K. Geim, K. S. Novoselov, and D. C. Elias, Proc. Natl. Acad. Sci. USA **110**, 3282 (2013).

[17] J. Hofmann, E. Barnes, and S. Das Sarma, Phys. Rev. Lett. **113**, 105502 (2014).

[18] N. Y. Astrakhantsev, V. V. Braguta, and M. I. Katsnelson, Phys. Rev. B **92**, 245105 (2015).

[19] I. Sodemann and M. M. Fogler, Phys. Rev. B **86**, 115408 (2012).

[20] J. E. Drut and T. A. Lähde, Phys. Rev. Lett. **102**, 026802 (2009); Phys. Rev. B **79**, 165425 (2009); **79**, 241405 (2009); J. E. Drut, T. A. Lähde, and E. Tölö, PoS Lattice **2010**, 006 (2010); **2011**, 074 (2011).

[21] S. Hands and C. Strouthos, Phys. Rev. B **78**, 165423 (2008); W. Armour, S. Hands, and C. Strouthos, *ibid.* **81**, 125105 (2010); **84**, 075123 (2011).

[22] P. V. Buividovich and M. I. Polikarpov, Phys. Rev. B **86**, 245117 (2012).

[23] P. V. Buividovich, E. V. Luschevskaya, O. V. Pavlovsky, M. I. Polikarpov, and M. V. Ulybyshev, Phys. Rev. B **86**, 045107 (2012).

[24] C. DeTar, C. Winterowd, and S. Zafeiropoulos, Phys. Rev. B **95**, 165442 (2017).

[25] C. DeTar, C. Winterowd, and S. Zafeiropoulos, Phys. Rev. Lett. **117**, 266802 (2016).

[26] M. V. Ulybyshev, P. V. Buividovich, M. I. Katsnelson, and M. I. Polikarpov, Phys. Rev. Lett. **111**, 056801 (2013).

[27] V. V. Braguta, S. N. Valgushev, A. A. Nikolaev, M. I. Polikarpov, and M. V. Ulybyshev, Phys. Rev. B **89**, 195401 (2014).

[28] T. O. Wehling, E. Sasioglu, C. Friedrich, A. I. Lichtenstein, M. I. Katsnelson, and S. Blugel, Phys. Rev. Lett. **106**, 236805 (2011).

[29] D. L. Boyda, V. V. Braguta, M. I. Katsnelson, and M. V. Ulybyshev, Phys. Rev. B **94**, 085421 (2016).